Available online at www.sciencedirect.com

SciVerse ScienceDirect

Ceramics International 39 (2013) 3731–3739

CERAMICS INTERNATIONAL

www.elsevier.com/locate/ceramint

Carbon doped TiO_2 nanotubes photoanodes prepared by *in-situ* anodic oxidation of Ti-foil in acidic and organic medium with photocurrent enhancement

Asma M. Husin Milad[a,b], Lorna Jeffery Minggu[a], Mohammad B. Kassim[a,c,*], Wan Ramli Wan Daud[a,b]

[a]*Fuel Cell Institute, Universiti Kebangsaan Malaysia, 43600 UKM Bangi, Selangor, Malaysia*

[b]*Department of Chemical and Process Engineering, Faculty of Engineering and Built Environment, Universiti Kebangsaan Malaysia, 43600 UKM Bangi, Selangor, Malaysia*

[c]*School of Chemical Sciences and Food Technology, Faculty of Science and Technology, Universiti Kebangsaan Malaysia, 43600 UKM Bangi, Selangor, Malaysia*

Received 13 September 2012; received in revised form 13 October 2012; accepted 16 October 2012
Available online 26 October 2012

Abstract

Carbon doped titanium oxide nanotubular arrays (C-TNT) were successfully fabricated in highly ordered arrays by *in-situ* anodic oxidation of titanium foil to enhance the photoelectrochemical performance of titanium oxide nanotubular arrays (TNT) under visible light. The carbon doped titanium oxide nanotube was achieved via an *in-situ* anodic oxidation of titanium foil at 20 V in acidic and organic media with 0.5 and 1 wt% carbon source (polyvinyl alcohol, PVA) at room temperature. The carbon was incorporated from PVA into the titanium oxide nanotubular arrays during the anodic oxidation process. FESEM micrographs of the nanotubular arrays of C-TNT showed uniform vertical nanotubes. The external shapes of the pores and structures of the nanotubular arrays of C-TNT were affected by the percentage of PVA in both of the electrolytes. The amounts of C incorporated into TNT increased linearly with the amount of PVA introduced into the electrolyte. The morphology of the C-TNT produced by *in-situ* doping is superior in terms of uniformity, and the nanotubes grow in the preferred *z*-direction compared to C-TNT obtained using a post doping technique. The influence of the carbon contents on the photocurrent densities of C-TNT photoanodes was tested in a photoelectrochemical cell, and the current–potential (*I–V*) profiles were established.

Keywords: TiO_2; Nanotubes; Anodic oxidation; Photoelectrode

1. Introduction

The semiconductor titania (TiO_2) is one of the best candidates for many applications, namely, photocatalysis [1,2], implant materials [3], hydrogen sensing [4], solar cells [5] and other electrochemical devices, due to its high efficiency in UV light, low cost, chemical inertness, ecofriendly nature and photostability [6,7]. However, the photocatalytic efficiency of TiO_2, which normally consists of rutile and anatase phases with a band gap of 3.0–3.2 eV, is very low under irradiation by sunlight [8,9]. The extension of the TiO_2 photoresponse to the visible wavelength region is crucial for its efficient use in photocatalysis applications. In recent years, much research has been focused on modifying the band gap of TiO_2 via doping processes, which will enable its photoresponse to be extended into the visible region [10–13]. Studies have been conducted on various transition metal cationic dopants [14,15], but it was discovered that they inhibit the photocatalytic activity of TiO_2. Non-metal dopants, such as nitrogen [10,16], fluorine [17], sulfur [12] and carbon [11,18–21] have been used to dope TiO_2 using various methods. The post doping of self-organized TiO_2 nanotubes with carbon by

*Corresponding author at: School of Chemical Sciences and Food Technology, Faculty of Science and Technology, Universiti Kebangsaan Malaysia, 43600 UKM Bangi, Selangor, Malaysia. Tel.: +60 3 89213980; fax: +60 3 89216024.

E-mail address: mbkassim@ukm.my (M.B. Kassim).

0272-8842/$ - see front matter © 2012 Elsevier Ltd and Techna Group S.r.l. All rights reserved.
http://dx.doi.org/10.1016/j.ceramint.2012.10.209

flame treatment has been reported to lead to a considerable photoresponse in the visible to near-IR region [19–22]. According to a study by Park et al., the post-doping with carbon by heating TiO_2 nanotubes in CO gas was reported to yield high aspect ratios and lead to good photoresponse in solar water splitting applications [20].

The photocatalytic efficiency of TiO_2 is highly dependent on the structure, such as nanoparticles, nanowires, nanorods, nanofibers and nanotubes. Nanotubular structures, which possess many special properties, have been reported to offer great potential in photoelectrochemical (PEC) applications [23–25]. The advantage of the nanotube structure is the large surface area afforded by both the inner and outer surfaces. Additionally, the use of nanotubes can enable electrons to have a directional flow and travel at a faster rate under an applied electric field. Several methods have been developed to produce titanium oxide nanotubes, such as a soft chemical process [26] and the deposition of titanium oxide onto alumina templates [27]. Nonetheless, to date, the anodic oxidation method is the easiest and simplest form of the soft chemical methods. Anodic oxidation involves the growth of oxides where the sample substrate is biased anodically with respect to a counter electrode in a specific electrolyte [18,28,29]. The highly ordered porous TiO_2 nanotubes grown directly from a titanium metal substrate by this method possess good uniformity, controllable pore size, good electronic conductivity and good mechanical adhesion strength. The sono-electrochemical anodic oxidation using an ethylene glycol–ammonium fluoride solution has been reported by Mohapatra et al. to produce carbon-doped TiO_2 nanotube arrays after annealing the as-anodized sample, which converts the amorphous nanotube arrays to a photoactive anatase phase. The carbon doping resulting from the reduction of ethylene glycol, which contains carbon, gives the TiO_{2-x} C_x [21].

In this work, we compared the C-TNT prepared by *in-situ* anodic oxidation in acidic electrolyte as in our previous work [18] with C-TNT prepared in organic electrolytes containing ethylene glycol with added polyvinyl alcohol (PVA). We explore an *in-situ* technique to introduce carbon dopant into TNT by the anodic oxidation of titanium foil in an acidic and organic medium with PVA as the carbon source. The influences of the medium used (i.e., an acidic or organic electrolyte) and the addition of PVA into the electrolyte on the nanotube films grown on titanium foil were studied in terms of the thickness, pore morphology and elemental compositions of the nanotube arrays. In addition, the effects on the photocurrent behavior of the nanotube films are reported.

2. Experimental work

2.1. Materials and chemicals

Titanium foil (Ti, 99.99%, Aldrich), polyvinyl alcohol ($[–CH_2CHOH–]_n$, +99%, hydrolyzed, Aldrich), ammonium fluoride (NH_4F, 98%, Merck), ethylene glycol ($C_2H_6O_2$, 99.5%, Merck), *ortho*-phosphoric acid (H_3PO_4, 85% in water, A&R marketing, UK) and sodium fluoride (NaF, 99.5%, Merck) were used as received. The aqueous solutions were prepared with high purity deionized water.

2.2. Preparation of C doped TiO_2 nanotubular array electrodes

Titanium foils (1.0 × 1.0 cm) with a thickness of 0.1 mm were cleaned via sonication in acetone, *iso*-propanol and ethanol successively. Then, they were rinsed with deionized water and dried under a nitrogen flow prior to the anodic oxidation process. The anodic oxidation was conducted in a two-electrode cell. The as-prepared sample with an exposed area of 0.64 cm^2 was used as the working electrode, and a platinum plate was used as the counter electrode. The distance between the two electrodes was kept at 2 cm in all experiments. The open circuit potential (OCP) of the cell was read before the potential was ramped to 20 V using a DC power supply (Agilent, E3631A) at 1 V s^{-1}. The electrolyte in the cell was stirred continuously throughout the anodic oxidation process for 45 min in all experiment sets. The time-dependent current behavior under this constant potential was recorded using a Fluke multimeter. The electrolytes for preparations of C doped TNT electrodes were described previously [18].

2.2.1. Preparation C-TNT in acidic electrolyte

The TiO_2 nanotubes were prepared in acidic electrolyte as previously described by Mohapatra et al. with some modifications [28]. The TNT and C-TNT arrays were grown via anodic oxidation on Ti foils in an acidic medium containing 0.5 M *ortho*-phosphoric acid, 0.14 M sodium fluoride and different amounts of PVA (0.5 and 1 wt%), and the pH of the electrolyte was 2.

2.2.2. Preparation C-TNT in organic electrolyte

The experimental procedures were adapted based on a method that was previously reported in the literature by Xie et al. with some modifications [29]. The TNT and C-TNT were grown using anodic oxidation of Ti foils in an aqueous electrolyte (DI water) consisting of 2 vol% ethylene glycol (EG), 0.3 wt% NH_4F and different amounts of PVA (0.5 and 1 wt%) and with a pH of 5.9.

2.3. Annealing of C doped TiO_2 nanotubular arrays

The anodized samples were annealed. This post-treatment process of C-TNT is vital for transforming the amorphous structure of titanium oxide into anatase crystalline material. Prior to the annealing step, the surface of the anodized samples was cleaned with deionized water to remove any ion residues, and the samples were dried under N_2 flow at 100 °C for 12 h. The C-TNT arrays were annealed in a muffle furnace (PyroTherm Furnace, EUROTHERM 91 e)

at 500 °C for 3 h in purified air, and the heating was programmed at a rate of 5 °C/min.

2.4. Morphological and surface structure characterization of C doped TiO_2 nanotubular arrays

The surface structure of the TNT and C-TNT arrays were investigated by field emission scanning electron microscopy (FESEM, ZEISS, SUPRA 55VD), and the elemental contents of the surfaces were determined by energy-dispersive X-ray analysis (OXFORD Instruments, INCA) at 40 V using Cu Kα radiation. The crystallinity of the anodized samples was established using the XRD spectra collected on a Bruker D8 Advance spectrometer in reflection mode with Cu Kα radiation (40 KV) equipped with a beam monochromator.

2.5. Photoelectrochemical test

The photoelectrochemical (PEC) test was performed in a standard three-electrode system with the TNT or C-TNT arrays as the working electrode (with an active area of 0.56 cm^2), a platinum plate as the counter electrode and an SCE as the reference. The electrochemical cell was equipped with a quartz window to allow a 450 W Xenon lamp at 100 mW/cm^2 intensity to illuminate the cell. The preparation of the TNT and C-TNT samples for PEC analysis has been described elsewhere [30]. The electrolyte (1 M KOH) was purged with nitrogen gas for 30 min prior to the tests, and the *I–V* curve was established at a scan rate of 50 mV s^{-1} using an Ametek Versastat 4 potentiostat.

3. Results and discussion

3.1. Anodic oxidation step

The current density transient was recorded during the anodic oxidation process for samples prepared in acidic (*ortho*-phosphoric acid/NaF) and organic (ethylene glycol/NH_4F) electrolytes (Fig. 1(a) and (b), respectively). A drastic decrease in the current that was recorded at the beginning of the anodic oxidation process corresponds to the formation of an oxide layer barrier of TiO_2 (high-field TNT formation with a thickness of 50 nm); The subsequent increase in the current at the applied constant potential resulted from the pitting of fluoride ions on the oxide layer before the current reached a steady plateau [31,32]. The mechanisms for the TNT and C-TNT materials are expected to be quite similar to those previously reported in the literature [31–33] because similar patterns were observed in both curves (Fig. 1a and b). The current density drastically decreases at the initial stage and then gradually stabilizes, finally reaching a steady stable plateau.

As shown in Fig. 1(a), the stabilized current density decreased with increased PVA concentration in the acidic electrolyte; conversely, as the PVA concentration increased, the stabilized current density increased in the organic

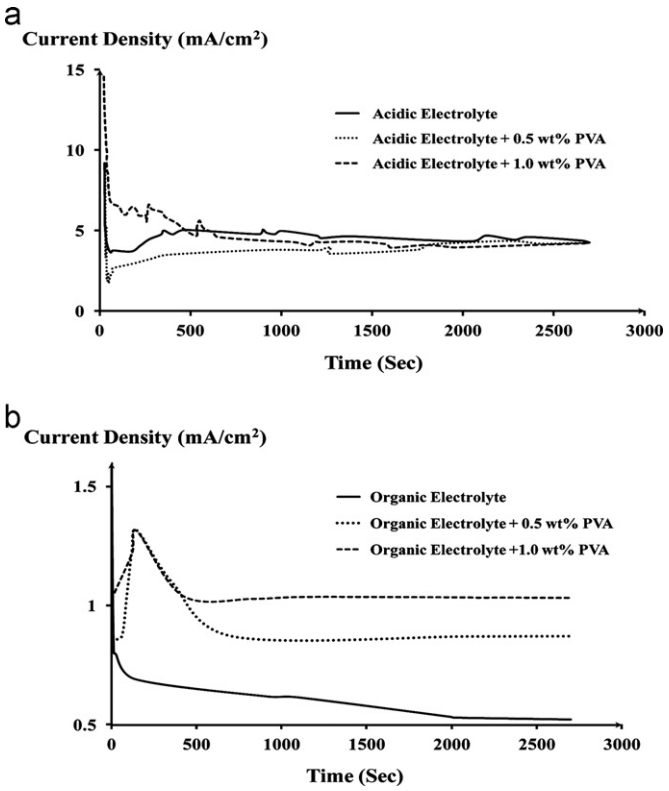

Fig. 1. Current density versus anodization time of Ti foil with 0, 0.5 and 1 wt% PVA in (a) acidic electrolyte and (b) organic electrolyte.

electrolyte (Fig. 1b). With increasing PVA content in the acidic and organic electrolytes, the current density decayed slowly and smoothly. This observation suggests that the PVA content in the electrolyte showed an inverse relationship with the flow of the anodized current density. The titanium foils in the electrolytes with varying amounts of PVA required a specific duration for the anodic oxidation process to form self-organized and ordered nanotube structures. The successful growth of the nanotubes was indicated when the current attained its plateau. The current density observed in the acidic electrolyte was higher than that in the organic electrolyte due to its high conductivity.

3.2. Morphology of C-TNT

At the present work, we fixed the anodization parameters as applied voltage, anodization time, composition of anodization electrolytes (acidic and organic) and pH, to study the effects of added PVA in both acidic and organic electrolytes on the morphology. But for comparison between the TNT prepared in acidic and organic electrolyte, the nature of electrolyte, content of F^- ions addition and pH were affected on the morphology. The nature of electrolyte played an important factor on the chemical dissolution rate of nanotubes layer, where the chemical dissolution rate in acidic electrolyte is higher than in the organic electrolytes. The mobility of F^- ions in acidic could be higher. So, in that case, the morphology of TNT

and C-TNT and the formation mechanism were different in both electrolytes.

The morphology of the as-produced TNT in acidic and organic electrolytes was shown in Fig. 2(a) and (b), respectively. The type of anodic oxidation electrolyte clearly plays an important role in the formation of the nanotubes in terms of the diameter and length of the tubes. The thickness of titania nanotube can be controlled by changing the anodization conditions which control the oxidation and the dissolution rates. Furthermore, the thickness of the nanotubes produced in the organic electrolyte was higher due to the lower dissolution rate. The organic electrolyte led to the formation of thicker walls of approximately 25–30 nm while the acidic electrolyte resulted in thinner walls of approximately 15–20 nm.

The average diameter and length of the tubes grown in the acidic electrolyte (Fig. 2a) were approximately 120 nm and 0.6 μm, respectively. The organic electrolyte produced tubes with smaller diameter at approximately 50 nm (Fig. 2b), and the tube body was relatively longer (approximately 3.5 μm) compared to that grown in the acidic electrolyte. These were similar to the results reported by Mohapatra et al. [28], Beranek et al. [34], and Macak et al. [35] and where the diameter of tubes prepared in acidic medium ranging from 90 nm to 130 nm and nanotube growth has been restricted to a length of 0.5–0.65 μm due to the strong chemical dissolution property of the titania layer into the electrolyte. However, Beranek et al. [34] reported for organic electrolyte the diameter of tubes ranging from 50 nm to 90 nm, and the lengths were 2–4.5 μm.

The shape of the undoped TNT prepared in acidic medium was completely different than the undoped TNT prepared in organic medium, where the shape of nanotubes prepared in acidic medium was formed in tapered conical shape (Fig. 2a) due to the strong etching of Ti foil by fluorine ion where it strongly adsorbed on Ti surface causing dissolution of the film even under open circuit potential conditions [36]. While the nanotubes prepared in organic medium have a stacked cylindrical shape (Fig. 2b) that was similar to the shape reported by Xie et al. [29].

The addition of PVA in both electrolytes led to different surface structures of TNT (Fig. 3a and b). Where, these additions affected slightly the dimension such as length, diameter and thickness especially in acidic medium (Table 1). The top surfaces of the C-TNT arrays prepared in the organic electrolyte with PVA were porous and uneven; the tubes were completely grown, but some of the tubes appeared to be blocked (Fig. 3b). In the acidic electrolyte, even with 1% PVA (Fig. 3a), the growth of the C-TNT arrays was complete without blockage at the top of the nanotube arrays, which had structures similar to those of the undoped TNT in the same medium (Fig. 2a). It

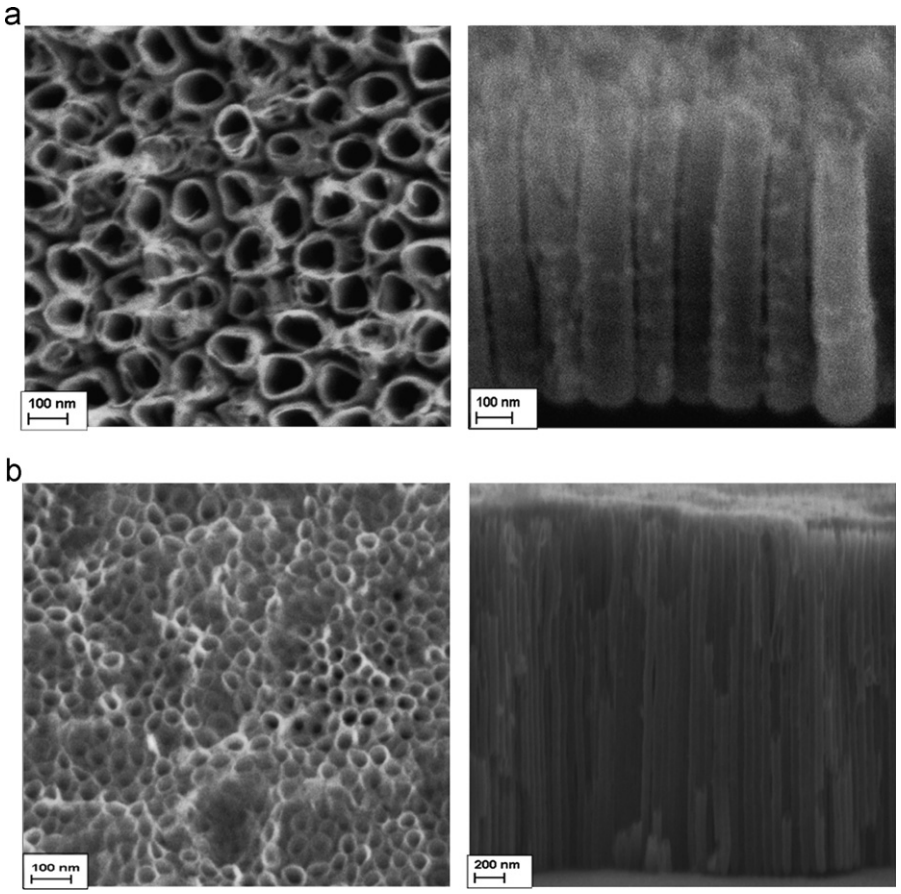

Fig. 2. Top surface and cross sectional views of TNT prepared by anodization of Ti foil in (a) acidic electrolyte and (b) organic electrolyte.

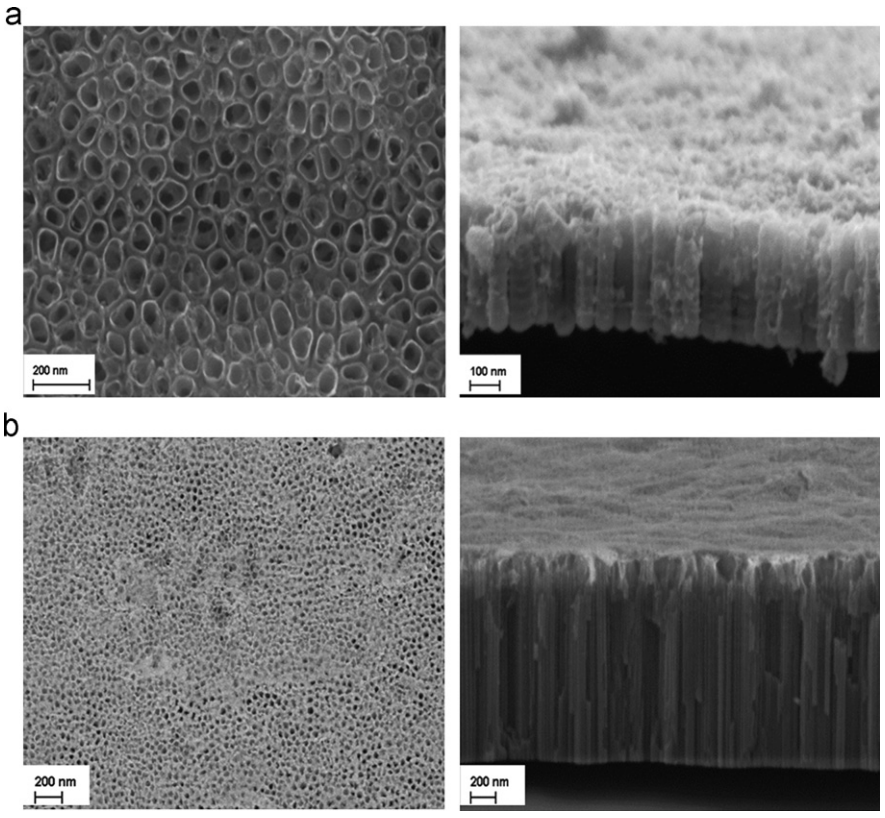

Fig. 3. Surface and cross sectional views of C-TNT prepared by anodization of Ti foil with 1 wt% PVA in (a) acidic electrolyte and (b) organic electrolyte.

Table 1
EDX data and the dimension sizes for C-TNT and TNT photoanodes.

	Photoanode using acidic electrolyte with wt% PVA			Photoanode using organic electrolyte wt% PVA		
	0	0.5	1	0	0.5	1
Carbon (at%)	0	2.43	2.76	2.14	7.59	8.45
Thickness (nm)	15–20	12–20	10–15	25–30	20–25	20–22
Inner diameter (nm)	120	125	130	50	45	35
Length (m)	0.6	0.5	0.55	3.5	3.45	3.55

is noted that the C-TNT grown from both media were in the preferred direction of the current flow, i.e. the *z*-direction. The addition of PVA was to increase the carbon content in both the electrolytes which lead to the increase of carbon incorporation to TNT during the anodization process. These observations demonstrate that the *in-situ* anodic oxidation technique has successfully produced a self-ordered titanium oxide nanotubular structure with or without the presence of PVA in the growth medium.

The EDX spectra of the undoped and *in-situ* doped C-TNT confirmed the presence of Ti, O and C (Fig. 4a and b). As shown in Table 1, the EDX results demonstrated that the carbon content on the surface of the doped TNT from the anodization process was in the range of 2.43–2.76% and 2.14–8.45% in the acidic and organic electrolyte, respectively. For anodization in the organic electrolyte without PVA, some carbon was still detected in the TNT because the organic electrolyte consisted of ethylene glycol, which acted as the source of carbon that could be incorporated into the TNT. As indicated in Table 1, the C content was found to increase uniformly with increasing amount of PVA in both electrolyte media. Table 2

The TNT adsorbed carbon species during the anodization process in both electrolytes and modified the tubes to $TiO_{2-x}C_x$ after annealing by internal diffusion of carbon into the lattice [28]. This route leads to improve the TNT photocurrent during photoelectrochemical water splitting, which was similar to the behavior of carbon modified TNT fabricated by flame pyrolysis [25] or a chemical vapor deposition method [20,37].

3.3. X-ray diffraction analysis

The degree of crystallinity and the crystal phases of the TNT and C-TNT of samples annealed at 500 °C were

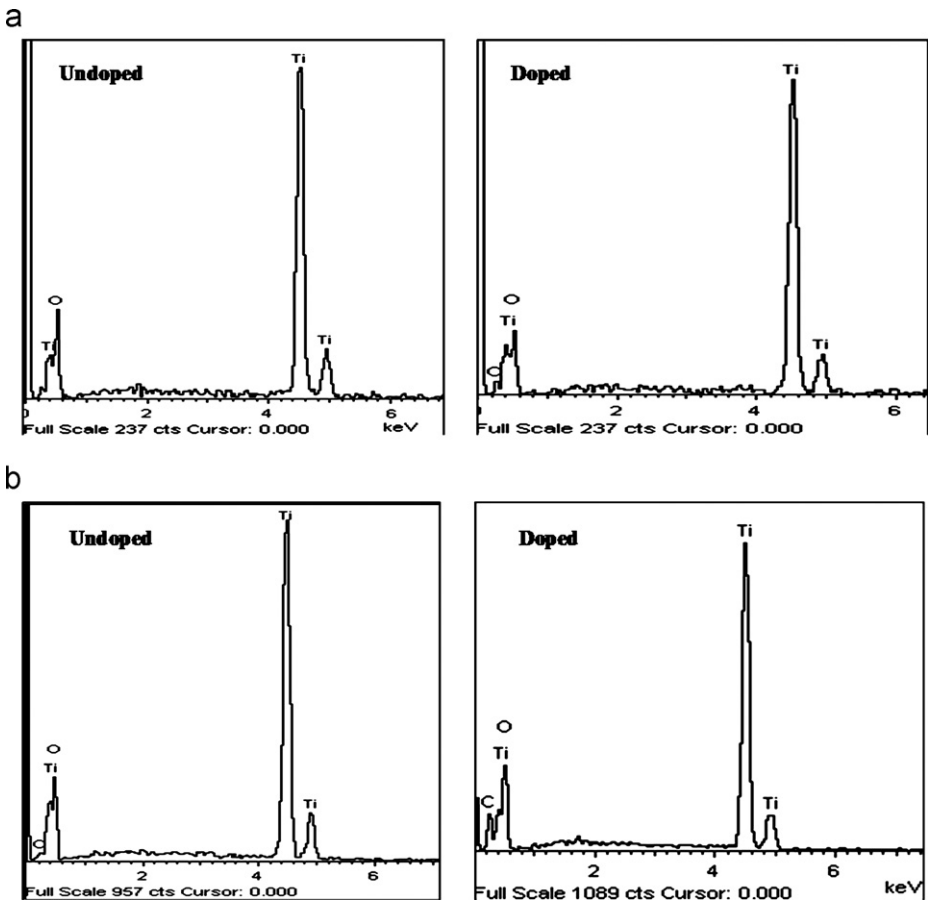

Fig. 4. EDX spectrum of the undoped and doped TNT prepared in (a) an acidic electrolyte and (b) an organic electrolyte.

Table 2
Comparison of photocurrent density (J) obtained from this work and other values reported in the literatures.

C-TiO_2 NTs	Carbon (at%)	Illuminated light (mW/cm^2)	Electrolyte of PEC	Potential (V)	J (mA/cm^2)	Ref.
C-TNT	62	300-W solar simulator	1 M KOH	0.2	1.35	[28]
				0.2	2.3	
1-step	0	AM 1.5, 100	1 M KOH	1	0.52	[32]
2-step	11.06			1	0.96	
C-doped TiO_2 NTs	na	100	1 M KOH	0.6	1.1	[40]
Short TNT	0.7	AM 1.5, 100	1 M KOH	1	0.05	[41]
Flame annealed short TNT	3.3				0.45	
Flame annealed long TNT	5.6				1.1	
Long TNT	3.5				1.05	
C-TNT in acidic +1 wt% PVA (short TNT)	2.76	100	1 M KOH	0.95	0.28	Present work
C-TNT in organic without PVA (long TNT)	2.14			1	0.3	

determined using the XRD diffractograms. All three phases, namely anatase, rutile and titanium, were present at the expected angles (Figs. 5 and 6), and the titanium peaks observed were attributed to the titanium substrate. All undoped and doped samples grown in the organic electrolyte exhibited a high degree of crystallinity, as shown in Fig. 5, but the doped sample in the acidic electrolyte showed no anatase peak (204) at 63° (Fig. 5a). The XRD patterns are in agreement with JCPDS file no. 01-083-0950. The crystalline phase was affected by the carbon content, which can be differentiated by the intensity of the peaks, as shown in Fig. 6(a) and (b).

3.4. Photoelectrochemical analysis

The photoelectrochemical measurements to obtain the photocurrent were conducted with a water splitting reaction using aqueous 1 M KOH as the reaction solution. Fig. 7 shows comparisons of the curves of the photocurrent density versus the applied potential for the TNT and

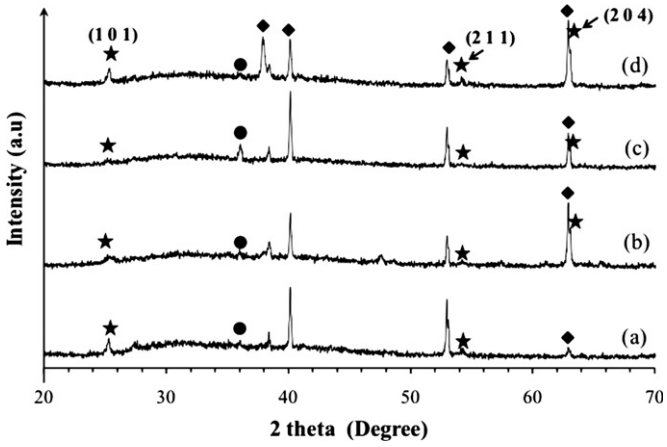

Fig. 5. XRD diffractogram of (a) pure TNTs in an acidic electrolyte, (b) pure TNTs in an organic electrolyte, (c) carbon doped TNTs in an acidic electrolyte with 0.5 wt% PVA and (d) carbon doped TNTs in an organic electrolyte with 0.5 wt% PVA [♦—Ti, ●—rutile, ★—anatase].

C-TNT photoanodes under xenon light illumination. The curves were classified based on the type of the electrolyte used to prepare the TNT and the PVA content. The dark and light currents produced were analyzed as a function of the applied potential in all samples. The dark current densities for all photoanodes were negligible. The photocurrent of TNT prepared in the organic electrolyte without PVA was higher than that of TNT prepared in the acidic electrolyte without PVA in the same test conditions, as shown in Fig. 7(a) and (d). The photocurrents of C-TNT prepared with PVA in both the acidic and organic electrolytes increased when the PVA concentration increased from 0.5% to 1% (Fig. 7). However, the photocurrent of C-TNT prepared with PVA in the acidic electrolyte (Fig. 7b and c) was higher than that of C-TNT prepared with PVA in the organic electrolyte (Fig. 7e and f). Although at bias above 0.95 V, the photocurrent for TNT without PVA prepared in organic electrolyte was higher than the C-TNT with PVA prepared in the acidic electrolyte (Fig. 7d). The photocurrent density of the undoped TNT produced without PVA in the acidic electrolyte was stable with applied bias (Fig. 7a). However, the photocurrent increased rapidly with the applied bias for TNT produced without PVA in the organic electrolyte (Fig. 7d).

For TNT prepared without PVA, the higher photocurrent for tubes prepared in organic electrolyte (Fig. 7d) could be attributed to the variation in the morphology of the nanotubes, where the long tubes grown in the organic electrolyte produced higher photocurrent densities than the shorter ones grown in the acidic electrolyte because of the higher surface area per unit volume, as deduced from the FESEM results (Fig. 2a and b) [38]. This difference can also be attributed to the presence of carbon in the TNT photoanode (Table 1) produced in the organic electrolyte without PVA because the carbon incorporation was due to the ethylene glycol during the anodic oxidation process as indicated in Section 3.2.

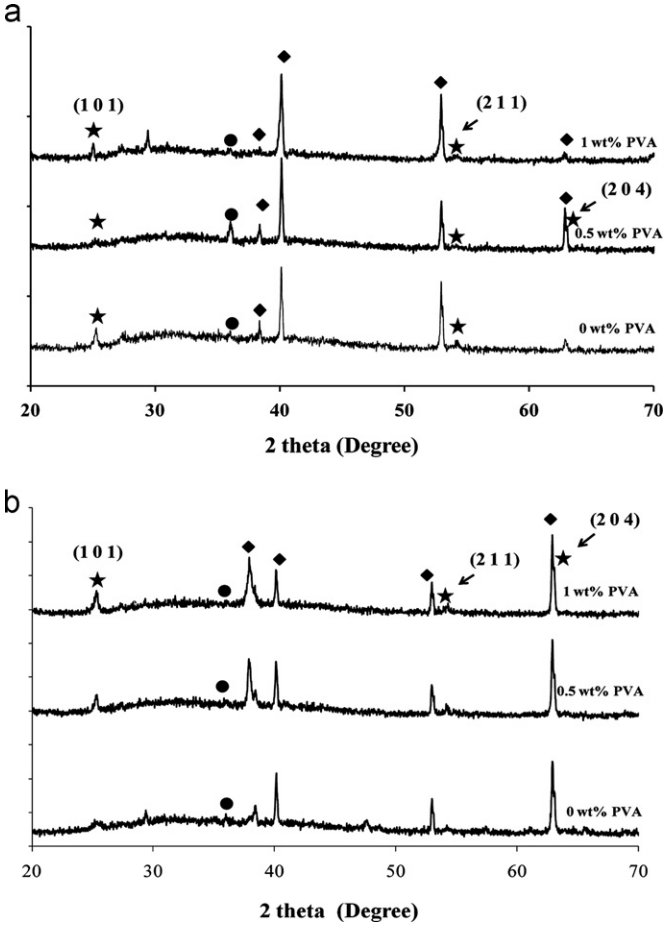

Fig. 6. XRD diffractogram of TNT with 0, 0.5 and 1 wt % of PVA as the carbon source in (a) an acidic electrolyte and (b) an organic electrolyte [♦—Ti, ●—rutile, ★—anatase].

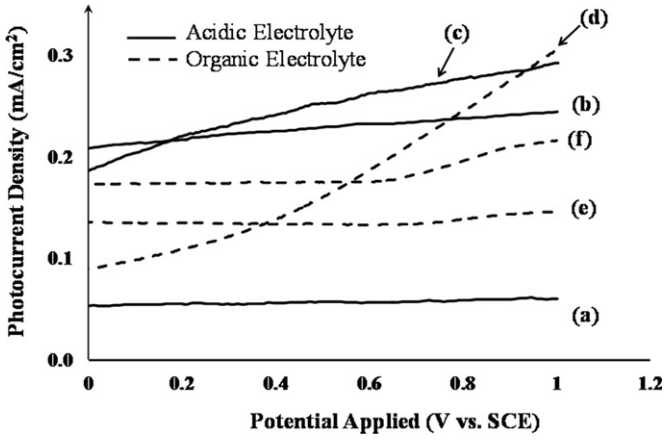

Fig. 7. Variation of the photocurrent density versus the measured potential for TNT prepared in (a) an acidic electrolyte, (b) an acidic electrolyte with 0.5 wt% PVA, (c) an acidic electrolyte with 1 wt% PVA, (d) an organic electrolyte, (e) an organic electrolyte with 0.5 wt% PVA and (f) an organic electrolyte with 1 wt% PVA under xenon light illumination in 1 M KOH electrolyte.

For preparation with PVA, the higher photocurrent for C-TNT prepared in acidic electrolyte could be attributed to the larger surface area due to the bigger diameter of

the nanotubes that facilitate reaction solution to enter the tube. The smaller diameter of the nanotube from the organic electrolyte with PVA seem to be blocked (SEM Fig. 3) which prevent reaction solution from getting inside the tube and this leads to lower photocurrent even though it has higher carbon content.

The highest photocurrent in this study was obtained by TNT prepared without PVA in organic electrolyte (Fig. 7d) after bias of 0.95 V. This can be attributed to the morphology of the nanotubes as well. Where, the TNT prepared without PVA in organic electrolyte have about double the inner tube surface area compared to C-TNT prepared with PVA in acidic electrolyte. Where TNT prepared without PVA in organic electrolyte produced long and thin nanotubes with 2.76% carbon content, and C-TNT prepared with 1% PVA in acidic electrolyte produced short and wide nanotubes with 2.14% carbon content. This is leading to the increase in surface area for reaction between TNT and reaction solution. Also the high voltage bias increased the separation rate of the photogenerated electron–hole pairs [39].

Below bias of 0.95 V, C-TNT prepared with 1% PVA in acidic electrolyte produced the highest photocurrent (Fig. 7c). Where, the recombination of the photogenerated electron–hole pairs was slow in TNT in organic electrolyte, due to the long tube compared to short C-TNT in acidic electrolyte and the carbon incorporation into TNT in acidic electrolyte enhanced the photoactivity of C-TNT photoanodes. The carbon doping of the titania has been reported to reduce the band gap of TNT [13]. Employing carbon dopants changed the optical response of TNT significantly as shown from the PEC results (Fig. 7) but the crystal structure and the dimension of C-TNT were only slightly affected (Figs. 2 and 3 and Figs. 5 and 6).

As shown in Fig. 7 and according to the carbon content in Table 1, the maximum photocurrent density was produced by C-TNT fabricated in the organic electrolyte without PVA (Fig. 7d) which produces the highest photocurrent of 0.3 mA/cm^2 under an anodic bias of 1 V (versus SCE). The best photocurrent density below 0.95 V bias was 0.28 mA/cm^2 obtained using C-TNT derived from a sample with 1.0 wt% PVA grown in an acidic electrolyte. The photocurrent values obtained in this study were similar to Zhang et al. [32] and Shankar et al. [41] with similar test conditions, however they had higher carbon content in the sample. Other photoelectrochemical results with C-TNT for water splitting produced higher photocurrent than our study because of the different conditions used such as bias voltage, light intensity, electrolyte, method of C-TNT preparation and carbon content [28,40,42]. For a nanotubes network structure, electron–hole pairs induced by photon absorption split more readily and in addition, produced a high photoanodic response that was attributed to the increased depth and better scattering of the light within the regular tube structure [43]. The photocurrent values were influenced by the carbon content in the TNT and by the nanostructures. The photocurrent in this study indicated that the C-TNT film has a behavior similar to that of an n-type semiconductor.

4. Conclusion

Highly ordered TNT arrays had been prepared by *in-situ* anodic oxidation of Ti foils in acidic and organic electrolytes with varying amounts of PVA additive as a carbon source at 20 V for 45 min. Both titanium oxide nanotube (TNT) and carbon doped titanium oxide nanotube (C-TNT) exhibited a high crystallinity after annealing at 500 °C and grew in the preferred orientation to the current flow. Approximately 2.75% and 8.45% carbon was incorporated into the TNT in the acidic and organic electrolyte, respectively. The diameters of the C-TNT prepared in acidic and organic electrolytes were 120 and 50 nm, with a corresponding length of 0.6 and 3.5 μm, respectively. The best photocurrent density below 0.95 V bais was obtained using C-TNT derived from a sample with 1.0 wt% PVA grown in an acidic electrolyte and was oxidized for 45 min. It was found that both the nanostructure and the C-content of the C-TNT contributed to the enhancement of the TiO_2 photoresponse.

Acknowledgment

The authors thank Universiti Kebangsaan Malaysia for providing the facilities and grants (UKM-GUP-BTT-07–30–190, UKM-OUP-TK-16–73/2010 and OUP-2012-073) and A.M.H.M thanks the Libyan government for the PhD scholarship.

References

[1] M.R. Hoffmann, S.T. Martin, W. Choi, D.W. Bahnemann, Environmental applications of semiconductor photocatalysis, Chemical Reviews 95 (1995) 69–96.
[2] A. Fujishima, K. Honda, Electrochemical photolysis of water at a semiconductor electrode, Nature 238 (1972) 37–38.
[3] S. Liu, A. Chen, Coadsorption of horseradish peroxidase with thionine on TiO_2 nanotubes for biosensing, Langmuir 18 (2005) 8409–8413.
[4] H. Li, L. Cao, W. Liu, G. Su, B. Dong, Synthesis and investigation of TiO_2 nanotube arrays prepared by anodization and their photocatalytic activity, Ceramics International 38 (2012) 5791–5797.
[5] V.S. Saji, H.C. Choe, W.A. Brantley, An electrochemical study on self-ordered nanoporous and nanotubular oxide on Ti–35Nb–5Ta–7Zr alloy for biomedical applications, Acta Biomaterialia 5 (2009) 2303–2310.
[6] G.K. Mor, K. Shankar, M. Paulose, O.K. Varghese, C.A. Grimes, Enhanced photocleavage of water using titania nanotube arrays, Nano Letters 5 (2005) 191–195.
[7] K. Zhu, T.B. Vinzant, N.R. Neale, A.J. Frank, Removing structural disorder from oriented TiO_2 nanotube arrays: reducing the dimensionality of transport and recombination in dye-sensitized solar cells, Nano Letters 7 (2007) 3739–3746.
[8] J.R. Bolton, Solar photoproduction of hydrogen: a review, Solar Energy 57 (1996) 37–50.
[9] V.M. Aroutiounian, V.M. Arakelyan, G.E. Shahnazaryan, Metal oxide photoelectrodes for hydrogen generation using solar radiation-driven water splitting, Solar Energy 78 (2005) 581–592.

[10] T. Morikawa, R. Asahi, T. Ohwaki, K. Aoki, Y. Taga, Band-gap narrowing of titanium dioxide by nitrogen doping, Journal Applied Physics 40 (2001) L561–L563.
[11] J. Lin, R. Zong, M. Zhou, Y. Zhu, Photoelectric catalytic degradation of methylene blue by C60-modified TiO_2 nanotube array, Applied Catalysis B: Environmental 89 (2009) 425–431.
[12] T. Umebayashi, T. Yamaki, H. Itoh, K. Asai, Band gap narrowing of titanium dioxide by sulfur doping, Applied Physics Letter 81 (2002) 454–456.
[13] K.S. Raja, M. Misra, V.K. Mahajan, T. Gandhi, P. Pillai, S.K. Mohapatra, Photo-electrochemical hydrogen generation using band-gap modified nanotubular titanium oxide in solar light, Journal of Power Sources 161 (2006) 1450–1457.
[14] K.E. Karakitsou, X.E. Verykios, Effects of altervalent cation doping of TiO_2 on its performance as a photocatalyst for water cleavage, Journal of Physical Chemistry B 97 (1993) 1184–1189.
[15] W. Choi, A. Termin, M.R. Hoffmann, The role of metal ion dopants in quantum-sized TiO_2: correlation between photoreactivity and charge carrier recombination dynamics, Journal of Physical Chemistry B 98 (1994) 13669–13679.
[16] J.L. Gole, J.D. Stout, C. Burda, Y.B. Lou, X.B. Chen, Highly efficient formation of visible light tunable $TiO_{2-x}N_x$ photocatalysts and their transformation at the nanoscale, Journal of Physical Chemistry B 108 (2004) 1230–1240.
[17] A. Hattori, M. Yamamoto, H. Tada, I. Seishiro, A promoting effect of NH_4F addition on the photocatalytic activity of sol–gel TiO_2 films, Chemistry Letters 27 (1998) 707–708.
[18] A.M. Milad, M.B. Kassim, W.R. Daud, Fabrication of carbon doped TiO_2 nanotubes via *in-situ* anodization of Ti-foil in acidic medium, World Academy of Science, Engineering and Technology 74 (2011) 171–175.
[19] R. Hahn, A. Ghicov, J. Salonen, V.P. Lehto, P. Schmuk, Carbon doping of self-organized TiO_2 nanotube layers by thermal acetylene treatment, Nanotechnology 18 (2007) ID:105604.
[20] J.H. Park, S. Kim, A.J. Bard, Novel carbon-doped TiO_2 nanotube arrays with high aspect ratios for efficient solar water splitting, Nano Letters 6 (2006) 24–28.
[21] S.K. Mohapatra, M. Misra, V.K. Mahajan, K.S. Raja, Design of a highly efficient photoelectrolytic cell for hydrogen generation by water splitting: application of $TiO_{2-x}C_x$ nanotubes as a photoanode and Pt/TiO_2 nanotubes as a cathode, Journal of Physical Chemistry C 111 (2007) 8677–8685.
[22] K. Shankar, M. Paulose, G.K. Mor, O.K. Varghese, C.A. Grimes, A study on the spectral photoresponse and photoelectrochemical properties of flame-annealed titania nanotube arrays, Journal of Physics D: Applied Physics 38 (2005) 3543–3549.
[23] M. Gratzel, Photoelectrochemical cells, Nature 414 (2001) 338–344.
[24] H. Wang, J.P. Lewis, Second-generation photocatalytic materials: anion-doped TiO_2, Journal of Physics: Condense Matter 18 (2006) 421–434.
[25] S.U.M. Khan, M. Al-shahry, W.B.I. Jr., Efficient photochemical water splitting by a chemically modified n-TiO_2, Science 297 (2002) 2243–2245.
[26] A.W. Tan, B. Pingguan-Murphy, R. Ahmad, S.A. Akbar, Review of titania nanotubes: fabrication and cellular response, Ceramics International 38 (2012) 4421–4435.
[27] M.S. Sander, M.J. Cotte, W. Gu, B.M. Kile, C.P. Tripp, Template-assisted fabrication of dense, aligned arrays of titania nanotubes with well-controlled dimension on substrate, Advanced Materials 16 (2004) 2052–2057.
[28] S.K. Mohapatra, M. Misra, V.K. Mahajan, K.S. Raja, A novel method for the synthesis of titania nanotubes using sonoelectrochemical method and its application for photoelectrochemical splitting of water, Journal Catalysis 246 (2007) 362–369.
[29] Z.B. Xie, S. Adams, D.J. Blackwood, Effects of anodization parameters on the formation of titania nanotubes in ethylene glycol, Electrochimica Acta 56 (2010) 905–912.
[30] A. Memar, W.R. Daud, S. Hosseini, E. Eftekhari, L.J. Minggu, Study on photocurrentof bilayers photoanodes using different combinations of WO_3 and Fe_2O_3, Solar Energy 84 (2010) 1538–1544.
[31] L. Taveira, J.M. Macak, H. Tsuchiya, L.F.P. Dick, P. Schmuki, Initiation and growth of self-organized TiO_2 nanotubes anodically formed in $NH_4F/(NH_4)_2SO_4$ electrolytes, Journal of Electrochemical Society 152 (2005) B405–B410.
[32] Z. Zhang, M.F. Hossain, T. Takahashi, Photoelectrochemical water splitting on highly smooth and ordered TiO_2 nanotube arrays for hydrogen generation, International Journal Hydrogen Energy 35 (2010) 8528–8535.
[33] J.W. Schultze, M.M. Lohrengel, D. Ross, Nucleation and growth of anodic oxide films, Electrochimica Acta 28 (1983) 973–984.
[34] R. Beranek, H. Tsuchiya, T. Sugishima, J.M. Macak, L. Taveira, S. Fujimoto, H. Kisch, P. Schmuki, Enhancement and limits of the photoelectrochemical response from anodic TiO_2 nanotubes, Applied Physics Letters 87 (2005) 243114.
[35] J.M. Macak, K. Sirotna, P. Schmuki, Self-organized porous titanium oxide prepared in Na_2SO_4/NaF electrolytes, Electrochimica Acta 50 (2005) 3679–3684.
[36] R.W. Schutz, D.E. Thomas, Corrosion of titanium and titanium alloys, Metals Handbook, Ninth edition, ASM International, 1987.
[37] A. Ghicov, J.M. Macak, H. Tsuchiya, J. Kunze, V. Haeublein, L. Frey, P. Schmuki, Ion implantation and annealing for an efficient N-doping of TiO_2 nanotubes, Nano Letters 6 (2006) 1080–1082.
[38] Y. Liu, J. Li, B. Zhou, J. Bai, Q. Zheng, J. Zhang, W. Cai, Comparison of photoelectrochemical properties of TiO_2-nanotube-array photoanode prepared by anodization in different electrolyte, Environmental Chemistry Letters 7 (2009) 363–368.
[39] N. Liu, I. Paramasivam, M. Yang, P. Schmuki, Some critical factors for photocatalysis on self-organized TiO_2 nanotubes, Journal of Solid State Electrochemistry (2012)http://dx.doi.org/10.1007/s10008-012-1799-z.
[40] S. Liu, L. Yang, S. Xu, S. Luo, Q. Cai, Photocatalytic activities of C–N-doped TiO_2 nanotube array/carbon nanorod composite, Electrochemistry Communications 11 (2009) 1748–1751.
[41] K. Shankar, M. Paulose, G.K. Mor, O.K. Varghese, C.A. Grimes, A study on the spectral photoresponse and photoelectrochemical properties of flameannealed titania nanotube-arrays, Journal of Physics D: Applied Physics 38 (2005) 3543–3549.
[42] S.E. John, S.K. Mohapatra, M. Misra, Double-wall anodic titania nanotube arrays for water photooxidation, Langmuir 25 (2009) 8240–8247.
[43] D. Chu, X. Yuan, G. Qin, M. Xu, P. Zheng, J. Lu, L. Zha, Efficient carbon-doped nanostructered TiO_2 (anatase) film for photoelectrochemical solar cells, Journal of Nanoparticle Research 10 (2008) 357–363.